Sensors & Actuators: B. Chemical 302 (2020) 127183

Contents lists available at ScienceDirect

Sensors and Actuators B: Chemical

journal homepage: www.elsevier.com/locate/snb

Online coupling of microchip electrophoresis with ion mobility spectrometry for direct analysis of complex liquid samples

Marián Masár[a,*], Jasna Hradski[a], Michaela Nováková[a], Roman Szucs[a], Martin Sabo[b], Štefan Matejčík[b]

[a] Department of Analytical Chemistry, Faculty of Natural Sciences, Comenius University in Bratislava, Mlynská dolina CH2, Ilkovičova 6, 842 15, Bratislava, Slovakia
[b] Department of Experimental Physics, Faculty of Mathematics, Physics and Informatics, Comenius University in Bratislava, Mlynská dolina F2, 842 48, Bratislava, Slovakia

ARTICLE INFO

Keywords:
Hyphenated techniques
Microchip electrophoresis
Ion mobility spectrometry
Carboxylic acids
Wastewater

ABSTRACT

This is the first report of coupling of microchip electrophoresis (MCE) with ion mobility spectrometry (IMS) for the analysis of liquid samples. Zone electrophoresis, employed on a microchip as a MCE technique, is suitable for coupling with IMS. Sample components separated electrophoretically in liquid phase were transferred from the microchip using auxiliary liquid. Direct liquid sampling interface was used for sample evaporation and introduction to IMS. In the IMS analyzer, the sample components were further separated in the gaseous phase. Online MCE-IMS coupling enabled acquisition of characteristic IMS response for the individual analytes. The proposed MCE-IMS technique was tested on a model mixture of a homologous series of carboxylic acids (formic acid, acetic acid, propionic acid, butyric acid, valeric acid and hexanoic acid) and subsequently applied to the analysis of wastewater sample obtained from a cattle farm. Total analysis time did not exceed six minutes regardless of the sample. Reproducibility of peak width in the MCE ranged from 0.56 to 1.95% RSD, while reproducibility of time of IMS response was in the range of 2.52–5.44% RSD for the studied carboxylic acids. RSD values of their reduced ion mobility were less than 0.56% for model and wastewater sample. Limits of detection ranged from 0.07 to 2.61 mg L^{-1}. The results clearly show the great analytical potential of developed MCE-IMS coupling for the analysis of complex liquid samples.

1. Introduction

Miniaturization as well as automation and simplification of the analytical processes represent main trends in the new analytical instrumentation research and development. Miniaturization of separation techniques enables reduction of the sample and working solutions (*e.g.*, buffers or mobile phase) volumes while also minimizing waste production. Compared to the conventional separation techniques, their miniaturized analogues offer faster response while reducing the cost of analysis [1]. Microchip electrophoresis (MCE), based on the same separation principles as CE, holds significant position among miniaturized separation techniques due to its relatively simple instrumental design [2]. On the other hand, downsizing leads to a reduction of separation path and i.d. of the channels, which restricts the applicability of MCE to the analysis of complex ionogenic samples due to the limited separation capacity and possible loss of detection sensitivity.

Various detection techniques have been coupled to the MCE in order to achieve a sensitive and selective response [3]. Some of the most widely used detection techniques include laser induced fluorescence [4], mainly due to its high sensitivity, and conductivity detection [5], due to its universality and straightforward miniaturization. In addition, amperometry [6], UV/Vis detection [7], chemiluminescence [8], electrochemiluminescence [9] and other unconventional detection techniques [10] have also been coupled to MCE. Introduction of MS, as a powerful identification technique coupled to the MCE enhanced its applicability in the analysis of multicomponent samples [11]. However, the combination of MS with MCE offers limited potential for miniaturization, and increases the cost of analysis. In addition, selection of buffers compatible with MS is also restricted.

In this context, ion mobility spectrometry (IMS) emerges as a possible detection technique for coupling with MCE mainly due to its fast response and relatively low cost [12]. IMS instrumentation was already

Abbreviations: MCE, microchip electrophoresis; IMS, ion mobility spectrometry; K_0, reduced ion mobility; DLS, direct liquid sampling; CC, coupled separation channels; PEEK, polyether ether ketone; MES, 2-(*N*-morpholino)ethanesulfonic acid; His, L-histidine; MHEC, methylhydroxyethylcellulose; RIP, reactant ion peak

* Corresponding author.
E-mail address: marian.masar@uniba.sk (M. Masár).

https://doi.org/10.1016/j.snb.2019.127183
Received 19 June 2019; Received in revised form 27 August 2019; Accepted 21 September 2019
Available online 25 September 2019

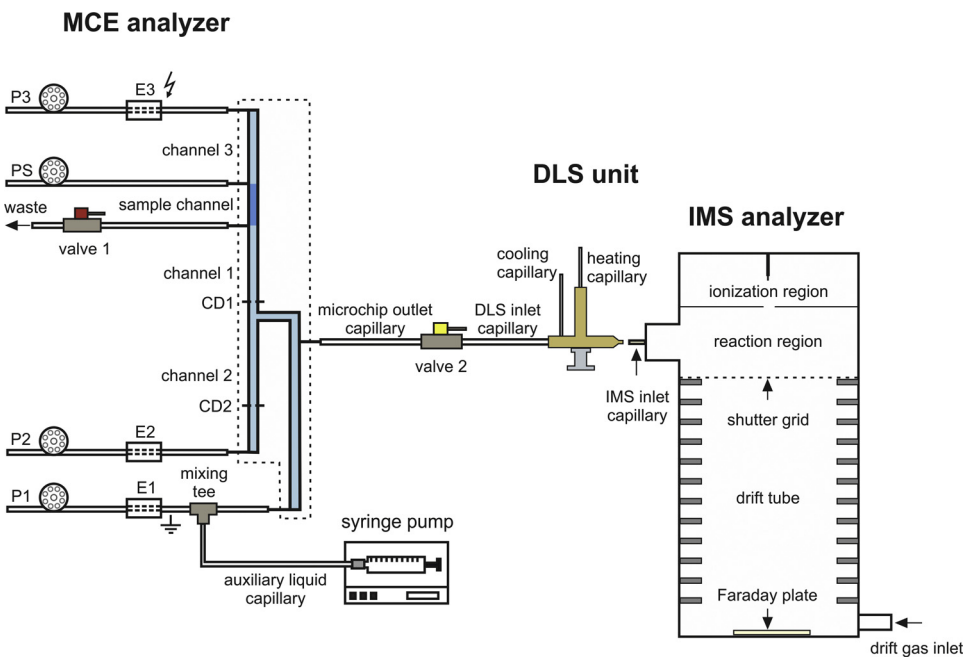

Fig. 1. Schematic diagram of the MCE-IMS coupling. P1, P2, P3, PS, peristaltic micropumps for filling microchip channels with buffer (channels 1, 2 and 3) and sample (sample channel) solutions; E1, E2, ground electrodes placed at the end of channels 1 and 2, respectively; E3, high voltage electrode placed at the end of channel 3; CD1, CD2, conductivity detectors placed in channels 1 and 2, respectively. The dashed line marks the microchip.

successfully miniaturized [13], which favors its coupling with MCE for example as a "lab-on-a-chip" application. At the same time, IMS is essentially a form of a separation technique, which can be beneficial for coupling with MCE when compared to conventional detection techniques. IMS was used as a separation technique prior to MS analysis [14].

Coupling of IMS with some other separation technique is preferable as it increases peak capacity and measurement sensitivity [15]. So far, combination of IMS with GC has the widest application. This coupling is relatively straightforward as the separation takes place in the gaseous phase in both of these techniques. GC-IMS was successfully applied to the analysis of volatile compounds in explosives, chemical warfare, biological and environmental samples [16–18]. Coupling of IMS with LC is almost exclusively used to improve selectivity of existing LC-MS systems [15]. Recently, thin layer chromatography was coupled to IMS for the separation of volatile and non-volatile compounds [19].

Analysis of liquid samples using IMS was first performed by the Hill group in 1989, they studied ESI as an introduction and ionization technique for IMS [20]. This led to development of the first CE-IMS coupling with several different ESI interface designs [21]. Despite achieving good separation efficiency and reproducibility of reduced ion mobility (K_0), the interfaces exhibited problems arising from an unstable spray, which increased overall noise of the system and decreased reproducibility of electrophoretic migration times. A similar study, conducted in 2011, focused on development of efficient ESI interface for coupling CE with IMS [22]. In addition, CE was also used as a preseparation technique prior to field asymmetric ion mobility spectrometry coupled to MS. This combination enabled significant reduction of the noise characteristics of MS and led to increased sensitivity [23,24].

In the early stages of development, IMS was referred to as gaseous electrophoresis [25], because it is based on the similar separation principle as CE. Coupling of MCE with IMS can be beneficial as it enhances identification potential of the MCE and resolving power of the IMS. Using K_0 values as a qualitative parameter, identification of the components can be accomplished after their MCE separation. This is applicable even in complex multicomponent samples, where component identification using conventional detection techniques coupled to MCE, based on migration time as a qualitative parameter, often fails. In addition, MCE-IMS coupling can provide significantly higher peak capacity than stand-alone IMS, which broadens the applicability of IMS in the analysis of complex samples. The different physical characteristics of the phases in which the separation is carried out presents the greatest challenge for coupling CE or MCE with IMS. This is probably one of the main reasons why despite similarity of these techniques only a few research papers have focused on coupling CE with IMS while MCE-IMS coupling, to the best of our knowledge, has not been reported so far.

Development of a suitable interface between liquid phase CE or MCE and gaseous phase IMS is essential for successful hyphenation of these techniques. Various techniques for introduction of liquid samples into IMS were developed and used, but most of them are suitable only for volatile or semi volatile compounds [26]. ESI offers the advantage of being both an introduction and ionization technique even for non-volatile compounds present in liquid samples. However, when implementing ESI to CE or MCE several challenges including consolidation of electrical circuits and selection of buffer(s) suitable for electrophoretic separation as well as creation of stable spray should be addressed [27].

Previously we have developed a direct liquid sampling (DLS) unit as a suitable interface for introduction of liquid samples into the IMS analyzer [28]. A DLS unit is based on the thermal spray, which in comparison with ESI eliminates the necessity for an additional volatile solution. A DLS unit is used for evaporation and subsequent introduction of the sample components into the IMS analyzer, where atmospheric pressure chemical ionization is applied.

In this paper we present a novel hyphenation of MCE and IMS instrument *via* DLS interface. Performance of developed MCE-IMS combination for two-dimensional separation of liquid samples is demonstrated on the separation of the first six carboxylic acids from a homologous series and analysis of wastewater sample for a content of these acids. In addition, miniaturized instrumentation used in this work has potential for portability and *in situ* analysis.

2. Material and methods

2.1. Instrumentation

MCE experiments were carried out on a poly(methyl methacrylate) microchip with coupled separation channels (CC; IonChip™ 3.0; Merck, Darmstadt, Germany). A CC microchip has integrated conductivity sensors, which were used for monitoring of separation directly on the microchip. The microchip was produced by hot embossing of the substrate and subsequent sealing with a thin plexiglass cover plate. The outer dimensions of the microchip are 68 mm x 25 mm x 3 mm. A

detailed description of the microchip production and dimensions of the channels can be found elsewhere [29,30]. Schematic arrangement of the microchip channels is shown in Fig. 1. The MCE analyzer (Department of Analytical Chemistry, Comenius University in Bratislava) included peristaltic micropumps (P1, P2, P3, PS) and membrane driving electrodes (E1, E2, E3). Peristaltic micropumps were used to transport buffer and sample solutions to the microchip channels. The specifics of the MCE analyzer can be found elsewhere [31]. Interconnection of the functional parts of the MCE analyzer is evident from Fig. 1.

A DLS unit was developed previously [28] and consists of a DLS inlet capillary for delivering the liquid sample to the DLS unit, a cooling capillary and a heating capillary (Fig. 1). The cooling capillary was used to supply atmospheric air at room temperature. The air flowing from the cooling capillary protected the DLS inlet capillary from overheating. The heating capillary was used to deliver heated atmospheric air. The heated air was mixed with air from the cooling capillary and liquid sample, which was subsequently evaporated at the tip of the DLS inlet capillary.

The IMS analyzer (Department of Experimental Physics, Comenius University in Bratislava in collaboration with MaSaTECH, Bratislava, Slovakia) was equipped with a corona discharge ionization source [28]. The sample entered the reaction region of the IMS analyzer where it was ionized. Subsequently, the sample was introduced into a drift tube through a Bradbury-Nielsen shutter grid. The signal of the ions detected on Faraday plate was amplified by a current amplifier and the IMS spectra were recorded by a control unit. The control unit was used for setting the operating parameters. The IMS control software (MaSaTECH) worked in both drift time and K_0 mode and was used to monitor IMS measurements. The IMS analyzer was calibrated using K_0 of 2,6-di-*tert*-butyl pyridine [32].

2.2. Device interconnection

The individual MCE and IMS equipment parts described above were connected to achieve IMS analysis of liquid samples after their MCE separation. Optimal parameters for the MCE-IMS coupling set-up on the MCE analyzer, DLS unit and IMS analyzer are summarized in Table 1.

Shut-off valves (IDEX Health & Science, Wertheim, Germany) were used to achieve proper filling of the channels as well as closing the inlets of the microchip. Valve 1 (i.d. 1 mm, volume 10 µL) was placed on the waste capillary of the MCE analyzer, while valve 2 (i.d. 0.5 mm, volume 2.5 µL) was located between the MCE analyzer and DLS unit. Two polyether ether ketone (PEEK) capillaries (IDEX Health & Science), the microchip outlet capillary (i.d. 0.178 mm) and the DLS inlet capillary (i.d. 0.254 mm) were joined by valve 2 and served as a connection for the MCE analyzer and DLS unit. A mixing tee made of PEEK (IDEX Health & Science) was located between E1 electrode and the microchip.

Table 1
Parameters of MCE and IMS analyzers and DLS unit.

Instrument	Parameter	Setting
MCE	operating mode	anionic
	driving current	25 µA
	effective separation path	59 × 0.2–0.5 × 0.14–0.2 mm (length × width × depth)
DLS	temperature of heating capillary	220 °C
	temperature of droplet stream	120 °C
	flow rate	20 µL min^{-1}
IMS	operating mode	negative
	drift field intensity	557 V cm^{-1}
	drift tube length	10.6 cm
	drift tube temperature	60 °C
	IMS operating pressure	600 mbar
	shutter grid pulse width	30 µs
	drift gas flow rate	600 mL min^{-1}
	sample gas flow rate	100 mL min^{-1}
	acquisition time	80 ms

An auxiliary liquid capillary (i.d. 0.127 mm) was used to connect a syringe pump (Cole-Parmer, Vernon Hills, IL, USA) to the mixing tee and subsequently to the microchip. A syringe pump with a 2.5 mL syringe (Hamilton, Bonaduz, Switzerland) was used to transfer the sample from the microchip to the DLS unit.

2.3. Chemicals, reagents and samples

Chemicals of p.a. purity, which were used to prepare buffer and model samples, were purchased from Merck (Darmstadt, Germany), Sigma-Aldrich (Steinheim, Germany) and Serva (Heidelberg, Germany).

For the preparation of the buffer and sample solutions, water purified through a Pro-PS system (Labconco, Kansas City, KS, USA) and then deionized by a Simplicity deionization unit (Millipore, Molsheim, France) was used. The buffer and sample solutions were refrigerated and used for a maximum of one week from the date of preparation. The buffer was filtered through membrane filters with a pore diameter of 0.8 µm (Millipore) prior to use.

The buffer used for MCE separations consisted of 10 mM 2-(*N*-morpholino)ethanesulfonic acid (MES) and 10 mM L-histidine (His) at pH 6.1. Standard solutions of C_1-C_6 carboxylic acids (formic acid, acetic acid, propionic acid, butyric acid, valeric acid and hexanoic acid) were prepared at a concentration of 1000 mg L^{-1}. A sample of wastewater taken from the cattle farm was centrifuged at 10,000 rpm. The supernatant was filtered through a membrane filter having a pore diameter of 0.45 µm (Millipore). Prior to analysis, the sample was diluted 100-fold with deionized water.

The microchip channels were filled daily with a 0.05% (v/v) methylhydroxyethylcellulose 30,000 (MHEC; Serva) solution for 5 min prior to the first analysis to suppress the EOF [33]. Subsequently, the channels were rinsed with deionized water and buffer for 10 min. Between the analyses, the microchip channels were only refilled with buffer and sample solutions for 2 min. After the last analysis the channels were rinsed with 2% (v/v) aqueous detergent solution (Extran MA 02, Merck, Darmstadt, Germany) for 5 min and deionized water for 5 min.

Atmospheric air purified by molecular sieve moisture trap (Agilent, Santa Clara, CA, USA) was used as a drift gas.

2.4. Measurement procedure

The microchip channels were first filled with corresponding buffer and sample solutions through four open inlets using peristaltic micropumps (Fig. 1). The filling procedure also included rinsing of the microchip channels. During this procedure valve 1 was open and valve 2 closed, which resulted in removing excess solution from the microchip to the waste container through valve 1. The rollers of the peristaltic micropumps closed the inlets to the microchip channels when the filling procedure ended. After filling had finished valve 1 was closed and subsequently valve 2 was opened. Afterwards a driving current was switched on and current flowed between the E1 and E3 electrodes. In the anionic mode of separation, anions were migrating from the sample channel towards the E1 electrode (currently used as an anode). The syringe pump was switched on and auxiliary liquid was pumped onto the microchip through the mixing tee in the direction opposite to the electrophoretic migration of the anions on the microchip. The auxiliary liquid was continuously moving towards the DLS unit through the only open outlet from the microchip. In this way, the separated components were removed from the microchip. In the DLS unit the separated sample components were evaporated. An outlet from the DLS unit was located directly in front of the IMS inlet capillary, which facilitated transfer of the sample components with minimal loss. Under given IMS working conditions (see Table 1) the sample was sucked into the reaction region of the IMS analyzer, where it underwent a reaction with the reactant ions. Further separation of ions continued in the IMS analyzer and detection on a Faraday plate took place.

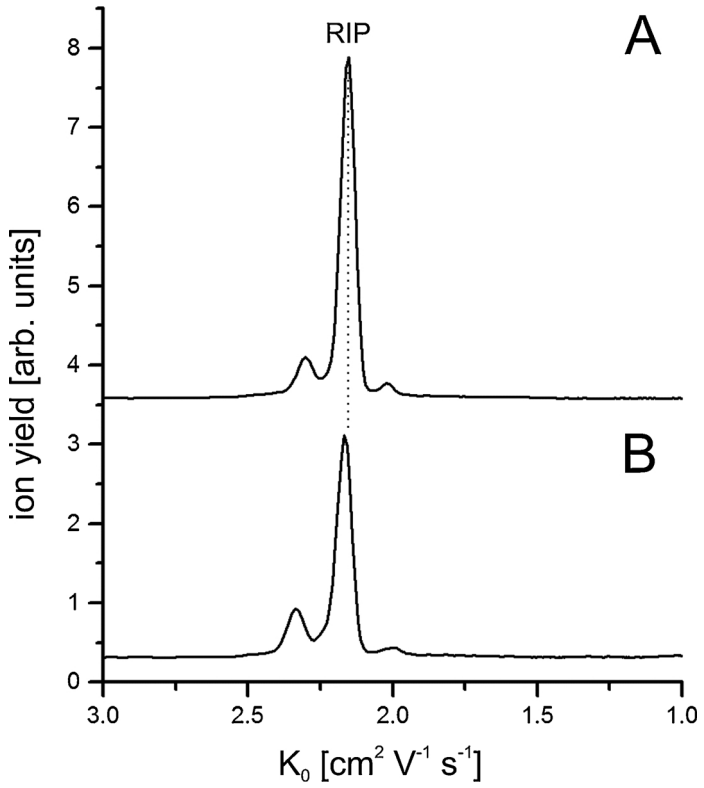

Fig. 2. IMS spectra of (A) drift gas and (B) 50% (v/v) MCE buffer prepared by diluting with deionized water. RIP, reactant ion peak.

2.5. Data processing

The experimental data were recorded using MicroITP software (conductivity data) and IMS control software (IMS data). The data obtained using MCE-IMS technique were presented as a 2D plot, where each point was characterized by the analysis time (given as the sum of the migration time, the time for the sample transfer from the microchip to the inlet of the IMS analyzer and the drift time), the K_0 value and the intensity of the ion yield. Data are represented as a heat map, where the K_0 value is set on the x-axis and analysis time on the y-axis and the signal intensity is indicated by the color (blue – minimum value; red – maximum value). The data were processed using Octave software (4.4.1). Prior to creation of the 2D plot all spectra were treated using a Savitzky-Golay filter.

3. Results and discussion

3.1. Development of MCE-IMS coupling

A key feature in developing the MCE-IMS technique is the transfer of the separated components from the microchip while minimizing dispersion and memory effect. Several different parameters affecting the MCE separation were optimized to reach fast separation and to implement hydrodynamic removal of the separated components from the microchip with minimal dispersion. To achieve this, an auxiliary liquid used for hydrodynamic removal was applied to the microchip and its compatibility with MCE was studied. The impact of auxiliary liquid on the electrophoretic separation was monitored by a contact conductivity detector placed directly on the microchip. In addition, we paid great attention to the transfer phenomena of the liquid through the DLS unit by controlling the temperature of the DLS unit as well as the flow rate of the auxiliary liquid, as these parameters can significantly affect separation on the microchip.

Two different applications of the auxiliary liquid to the microchip were tested, co-flow and counter flow, having the same or opposite direction to the electrophoretic transport of the separated components on the microchip, respectively. A counter flow arrangement was preferred because of the shorter analysis time when compared to when co-flow was employed. In the counter flow arrangement, the syringe pump was connected perpendicular to the separation path. The separated components were transferred from the microchip after detection by a conductivity detector, which was placed at the end of channel 1 (Fig. 1). Using the counter flow, transfer of each component from the microchip to the DLS unit was reached within one minute.

3.2. Optimization of MCE-IMS parameters

CC microchip enables employment of various electrophoretic techniques and their (mutual) combinations as well as opening and closing of the microchip inlets or outlets based on the current needs [34]. In this study, separations were carried out in channel 1, *i.e.*, current was flowing between the E3 and E1 electrodes (Fig. 1). A conductivity detector located at the end of channel 1 was used to monitor the electrophoretic separations on the microchip.

Electrophoretic separations were performed in a hydrodynamically closed system. This led to the necessity of suppressing EOF, otherwise separation efficiency would be dramatically decreased, which results in poor resolution [34]. Dynamic coating of microchip channels was used to suppress EOF. This was carried out by daily filling the microchip channels with a 0.05% (v/v) solution of MHEC for a period of at least 5 min prior to the first analysis [33]. Using this procedure, we avoided the problems associated with the clogging of the heated DLS inlet capillary (Fig. 1) by this polymer. Among various electrophoretic techniques, zone electrophoresis was chosen for the MCE-IMS coupling. In zone electrophoresis, analytes are distributed into individual zones which are spatially separated by buffer. This provides a good basis for the subsequent introduction of the separated components into the IMS.

Because electrophoretic separations take place in buffer medium, separated analytes have to be transferred to IMS together with buffer components. In this context, different buffers were tested for efficient

electrophoretic separation, and at the same time, for minimal effect on the response of the sample components in the IMS. Widely used buffer consisting of MES and His was chosen for electrophoretic separations of anions. A value of pH 6 was selected as at this pH maximum differences in effective mobilities of all analytes were observed. Under these conditions, electrophoretic separations are based on differences in actual ionic mobilities of the acids [35]. By comparing IMS spectra (see Fig. 2) it is evident that this buffer met the necessary IMS requirements, since it exhibited only a slightly reduced response when compared to the drift gas.

In order to assess the effect of the auxiliary liquid composition on zone dispersion, different auxiliary liquids were tested including buffers typically used in MCE separations under selected pH conditions. Composition of the auxiliary liquid affected mainly the rate of zone dispersion of the sample components on the microchip as well as in the microchip outlet capillary. Buffer, used for the MCE separation, diluted to 50% with deionized water was chosen as the most suitable auxiliary liquid because (1) it did not interfere with the MCE separation since its conductivity was high enough not to interrupt the high voltage applied through the separation path, (2) it allowed low dispersion transfer of the components separated by the MCE to the DLS unit, and (3) it did not interfere with the response of the studied analytes in the IMS analyzer. The IMS spectrum of 50% (v/v) buffer is shown in Fig. 2B.

DLS parameters were optimized mainly to minimize negative impact on the MCE separation expressed as resolution, baseline stability and noise characteristics. One of the most important parameters proved to be the temperature of the droplet stream exiting from the DLS unit, which was tested in the range of 110–170 °C. The choice of temperature range was limited on one hand by the need for evaporation of the sample, and by heat resistance of the DLS inlet capillary on the other. Although higher temperatures are generally more favorable, frequent blockages of the DLS inlet capillary were observed. Also, slightly lower temperature prevents thermal degradation of analytes, which led to choosing 120 °C as the optimal temperature for the droplet stream. In addition, the flow rate of the auxiliary liquid is a very significant parameter which affects the quality of MCE separation. In our experience, a flow rate of 20 μL min^{-1} was chosen to minimize peak dispersion of the transferred components and, at the same time, to eliminate a negative impact on the response of the conductivity detector placed on the microchip.

IMS parameters were optimized mainly to achieve stable, reproducible and sensitive response from the IMS analyzer. Temperature of the drift tube plays a key role in sensitivity and selectivity of the IMS, especially in the case of analysis of liquid samples. Temperature was tested in the range of 60–110 °C. With increasing temperature resolving power decreased, while sensitivity increased. A temperature of 60 °C was selected as a compromise between the sensitivity and selectivity. Pressure in the drift tube affects both resolution and sensitivity. Pressure was tested in the range of 500–800 mbar. Although higher peak intensities were observed at lower pressure, this led to decrease in the resolution of the analytes. A pressure of 600 mbar was selected as optimal regarding the sensitivity and resolution. In order to achieve sensitive response width of the shutter grid pulse was tested in the range of 10–60 μs. Since increase in the peak height leads to decrease in resolution a 30 μs shutter grid pulse width was chosen as optimal due to relatively high intensity and low impact on the resolution.

3.3. MCE-IMS analysis of model sample

A model sample containing C_1-C_6 straight-chain carboxylic acids was chosen to show the potential of the developed MCE-IMS coupling. Results from the MCE separation of a model sample using conductivity detection on the microchip are shown in Fig. 3A. The 2D plot in Fig. 3B represents results achieved using the MCE-IMS technique. The use of MCE-IMS coupling led to time evolution of IMS response, which is a result of the gradual introduction of individual components into IMS after MCE separation on the microchip.

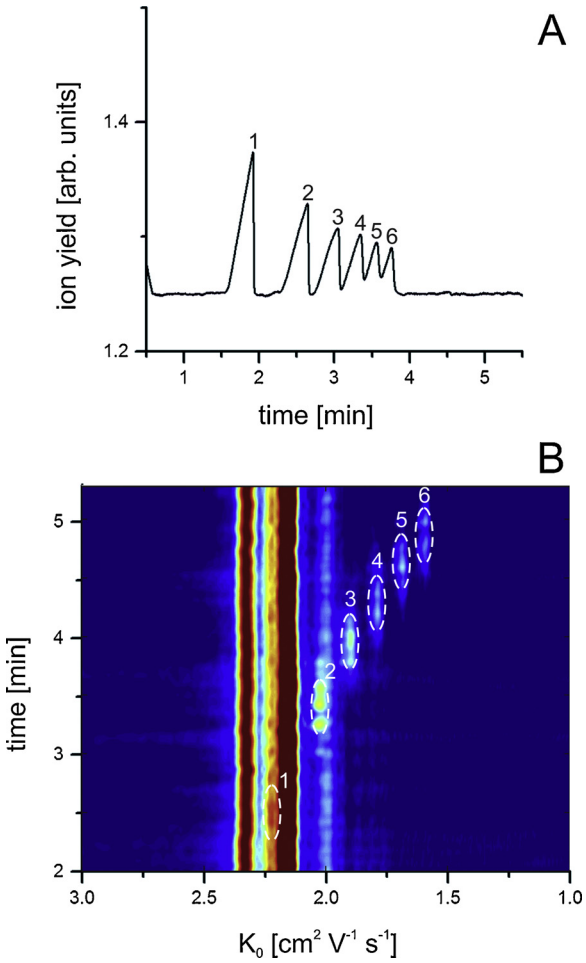

Fig. 3. MCE-IMS analysis of model sample of C_1-C_6 carboxylic acids monitored by (A) contact conductivity detector on the microchip and (B) IMS analyzer. Model sample contained 10 mg L^{-1} of all studied analytes. 1, formic acid; 2, acetic acid; 3, propionic acid; 4, butyric acid; 5, valeric acid; 6, hexanoic acid.

The MCE-IMS coupling enabled a successful transfer of the separated components from the microchip to the IMS analyzer. The time delay between responses of the acids from the conductivity detector on the microchip and the IMS analyzer was approximately one minute. Comparison of overall detection time windows of all studied components on the microchip (2.32 min) and in the IMS analyzer (2.90 min) shows an approximately 25% increase in time for IMS response.

In Table 2 average migration times in the MCE, the average peak width in the MCE from the conductivity detector, *i.e.*, time of passing

Table 2
Repeatability of migration times and dispersion parameters of analytes transferred from MCE to IMS.

Analyte[a]	MCE Migration time [min] (RSD [%])[b]	Peak width [min] (RSD [%])[b]	IMS Response time [min] (RSD [%])[b]	Dispersion [%]
Formic acid	1.92 (0.42)	0.42 (1.10)	0.45 (3.38)	106
Acetic acid	2.64 (0.55)	0.41 (0.56)	0.47 (2.52)	115
Propionic acid	3.04 (0.51)	0.37 (0.73)	0.46 (2.56)	126
Butyric acid	3.35 (0.44)	0.30 (1.19)	0.40 (2.78)	131
Valeric acid	3.56 (0.48)	0.22 (1.17)	0.30 (4.68)	133
Hexanoic acid	3.76 (0.39)	0.24 (1.65)	0.34 (5.44)	144

[a] Analytes present in the model sample, each at 10 mg L^{-1} concentration.
[b] Number of repetitions, $n = 5$.

through the detector, and average time of the IMS response are summarized for all six model sample components prepared at 10 mg L^{-1} concentration. RSD values of migration time in the MCE for model sample components were less than 0.6%. RSD values of peak width in the MCE (0.6–1.7%) and time of the IMS response (2.5–5.4%) calculated from 5 repeated runs indicated good repeatability.

Dispersion was calculated from average peak width in the MCE and time of the IMS response. Based on the data in Table 2, it is evident, that dispersion is increased for later migrating components, which indicates, that diffusion is a significant dispersion phenomena. The average value of the transfer dispersion, when taking into account all studied analytes is approximately 25%. This can be explained by the fact that transfer from MCE to IMS was realized by the hydrodynamic flow of auxiliary liquid, which is characterized by a parabolic flow profile. Nevertheless, this did not significantly affect the separation of C_1-C_6 carboxylic acids, as evident from Fig. 3B.

Standard procedure was used for calculation of the limit of detection (LOD) based on 3.3 times of the standard deviation of the blank to the slope of the calibration curve using the peak height [36]. Limit of quantitation (LOQ) was calculated based on 10 times of the standard deviation of the blank to the slope of the calibration curve [36]. LODs ranged from 0.07 to 2.61 mg L^{-1}, while LOQs were in the range of 0.20–7.92 mg L^{-1} (Table 3). Good linearity between the peak height from the IMS response and concentration of the analyte can be observed in the range from 1.5 to 25 mg L^{-1} for most of the studied analytes ($R < 0.993$).

The samples were ionized by chemical ionization in IMS. The reactant ion peak (RIP; K_0 of 2.16 cm^2 V^{-1} s^{-1}) is composed of $O_2^-(H_2O)_n$ [37]. The reactant ions ionize the sample components *via* electron transfer reactions:

$$O_2^- + M \rightarrow M^- + O_2$$

where M is the sample component. This ionization reaction is very efficient providing that the electron affinity of M exceeds the electron affinity of O_2 (0.448 ± 0.006) [38], which is the case for the studied components.

Characteristic peaks were formed for all six model sample components after the MCE-IMS analysis. The K_0 values obtained using the MCE-IMS technique as well as K_0 values found in the literature are summarized in Table 4. RSD values of K_0 obtained using MCE-IMS analysis ranged from 0.37–0.53% for model sample. As evident from Table 4, K_0 decreased with the increase in the carbon chain length.

An effect of buffer components on the K_0 values of model sample components was studied by direct introduction of individual standard solutions to the IMS. This enabled acquisition of another set of K_0 values measured under the same IMS conditions (Table 4). By comparing these results with those obtained from MCE-IMS analysis, it is evident that K_0 values were not affected by the buffer used for the MCE separation and the auxiliary liquid. In addition, RSD values of K_0 obtained using direct IMS analysis ranged from 0.24–0.32% and did not significantly differ from those obtained from MCE-IMS analysis.

At the same time, K_0 values of the carboxylic acids achieved in this study are in good agreement with those reported in the literature, when air was used as a drift gas [39]. Although the K_0 values are normalized to the standard temperature (273 K) and pressure (1013.25 mbar, corresponding to 760 torr), they are also dependent on the drift gas composition as well as the electric field [39]. This can lead to small differences in K_0 values, when different drift gases are used, as evident from Table 4 [40,41].

Table 3
Limit of detection, limit of quantitation and linear range of C_1-C_6 carboxylic acids using MCE-IMS.

Analyte	LOD [mg L^{-1}]	LOQ [mg L^{-1}]	Linear range [mg L^{-1}]
Formic acid	2.61	7.92	5.0 – 25.0
Acetic acid	0.07	0.20	0.2 – 25.0
Propionic acid	0.56	1.69	1.5 – 25.0
Butyric acid	0.51	1.54	1.5 – 25.0
Valeric acid	0.39	1.17	1.5 – 25.0
Hexanoic acid	0.54	1.63	1.5 – 25.0

LOD, limit of detection; LOQ, limit of quantitation.

3.4. MCE-IMS analysis of wastewater sample

The developed method was applied to the analysis of wastewater from cattle farm. The presence of C_1-C_6 carboxylic acids can be expected in these types of samples because of anaerobic biodegradation of organic matter. In general, samples of biological origin usually contain various ionogenic components that can be present at relatively high concentration levels, *e.g.*, chloride and sulfate (Fig. 4). These can co-migrate with the studied analytes, especially when a microchip with a short separation path is used.

We have applied only minimal sample pretreatment prior to the MCE-IMS analysis, including filtration and dilution. Such simple preparation of multicomponent sample was chosen to show the benefits of the developed coupling and the limitations of the MCE microchip when used with a universal detection technique. As evident from the electropherogram in Fig. 4A, the use of a microchip with conductivity detection in the analysis of a wastewater sample is restricted in terms of separation as well as detection selectivity. Although a MCE microchip was sufficient for the separation of a model sample of C_1-C_6 carboxylic acids (Fig. 3A), analysis of a wastewater sample without further pretreatment has led only to poor resolution of individual components on the microchip (Fig. 4A).

Repeatability of migration times in MCE for acetic acid present in the wastewater sample (2.95 min average migration time, 0.74% RSD) was similar to that in the model sample (0.55% RSD; Table 2). However, slight shift in the average value of migration times can be observed when comparing model to the wastewater sample, 2.64 and 2.95 min, respectively. This can be assigned to matrix effects from the wastewater sample, where various additional ionogenic components can be present in the sample. Migration time of valeric, isovaleric and hexanoic acid in the wastewater sample can be only estimated from the MCE with conductivity detection, given that they migrate unresolved in one peak (3.63 min average migration time, 0.85% RSD).

The 2D plot from the analysis of the wastewater sample using the MCE-IMS technique is shown in Fig. 4B. Three of the studied analytes, acetic acid, valeric acid and hexanoic acid, were positively identified in the wastewater sample using the MCE-IMS technique, based on the K_0 values and a standard addition method. RSD values of K_0 obtained using MCE-IMS analysis ranged from 0.49–0.56% for wastewater sample. Average K_0 values of C_1-C_6 straight-chain carboxylic acids in the wastewater were the same as those in the model sample, which implies a minimal sample matrix effect on the K_0 values (Table 4). This demonstrates the advantage of MCE-IMS techniques applied to the analysis of wastewater sample, or multicomponent ionogenic sample in general when compared to the MCE with conductivity detection as it offers unique identification of the analytes based on K_0 values.

As evident from Fig. 4B, an additional sample component with K_0 of 1.66 cm^2 V^{-1} s^{-1} was detected in the wastewater sample. Based on relatively close K_0 values of this component to those of valeric acid, we assumed that this could be an isomeric form of valeric acid. This was confirmed by standard addition of isovaleric acid to the sample analyzed.

Concentrations of the analytes in wastewater sample were calculated from the peak height. As the peaks of the analytes were overlapped on the response from conductivity detector, only IMS response could be used for quantitation. Concentrations were determined as follows: acetic acid (1065.4 ± 53.3 mg L^{-1}), valeric acid (392.2 ± 13.8 mg L^{-1}), isovaleric acid (806.2 ± 41.9 mg L^{-1}) and

Table 4
The reduced mobilities K_0 [$cm^2\ V^{-1}\ s^{-1}$] (RSD [%]) of analytes obtained in this work compared with published data.

Analyte	Drift gas: air				Drift gas: N_2	
	MCE-IMS[a] Model sample	IMS[a] Model sample	MCE-IMS[a] Waste water	Ref. [39]	Ref. [40]	Ref. [41]
Formic acid	2.23 (0.37)	2.24 (0.24)	–	–	–	2.66
Acetic acid	2.04 (0.41)	2.04 (0.27)	2.05 (0.56)	2.03	2.18	2.32
Propionic acid	1.90 (0.37)	1.90 (0.29)	–	1.94	1.86	–
Butyric acid	1.79 (0.47)	1.80 (0.25)	–	–	1.75	–
Valeric acid	1.69 (0.42)	1.69 (0.32)	1.71 (0.49)	–	1.64	–
Hexanoic acid	1.59 (0.53)	1.60 (0.28)	1.57 (0.53)	–	1.56	–

[a] Number of repetitions, $n = 5$.

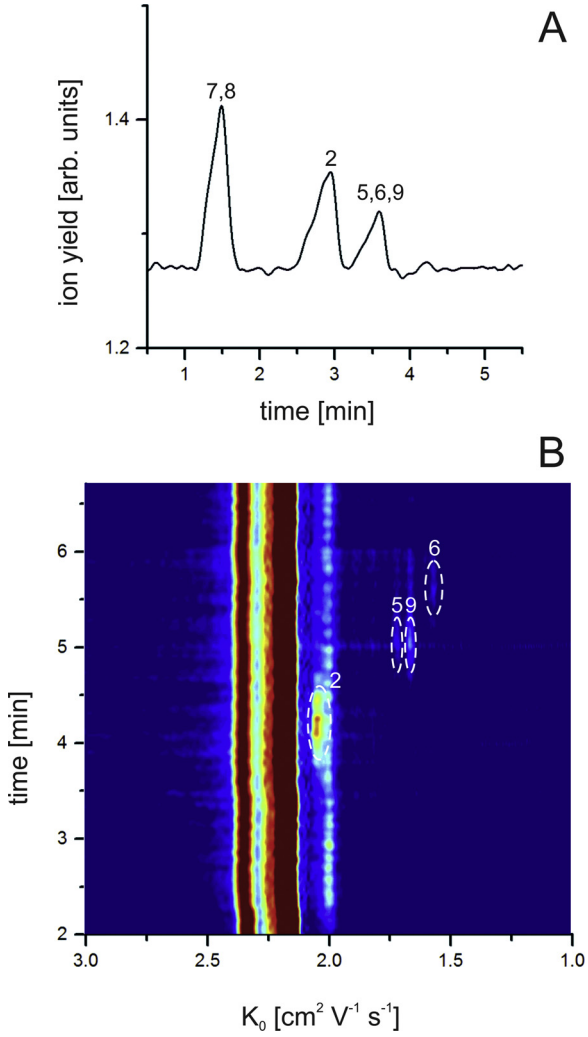

Fig. 4. MCE-IMS analysis of wastewater sample monitored by (A) contact conductivity detection on the microchip and (B) IMS analyzer. Wastewater sample was 100-fold diluted with deionized water. 2, acetic acid; 5, valeric acid; 6, hexanoic acid; 7, chloride; 8, sulfate; 9, isovaleric acid.

hexanoic acid (395.7 ± 12.3 mg L^{-1}).

These results clearly show the advantage of MCE-IMS coupling for the analysis of complex liquid samples when their individual separation and identification power is not sufficient to reach successful resolution of the components.

4. Conclusions

In the present paper, we have demonstrated for the first time successful online MCE-IMS coupling using the DLS interface between MCE (liquid phase) and IMS (gaseous phase). In the developed MCE-IMS hyphenation we have (1) implemented the auxiliary liquid to the microchip without disturbing the MCE separation, and at the same time (2) employed the same buffer for the MCE separation and as the auxiliary liquid.

The developed MCE-IMS technique was applied to the analysis of a model sample of C_1-C_6 linear carboxylic acids. IMS response of all components separated by MCE was observed and total analysis time including both MCE and IMS stages did not exceed six minutes. Additionally, the applicability of MCE-IMS technique was demonstrated in the analysis of wastewater. The presence of acetic acid, valeric acid, isovaleric acid and hexanoic acid was confirmed in the wastewater based on the K_0 values. This clearly shows the great potential of the developed coupling in the analysis of complex liquid samples. Such types of samples require the use of highly efficient separation technique characterized by high peak capacity. Overall peak capacity of the newly developed two-dimensional technique is very favorable (some thousands), taking into account that, in theory, peak capacity of MCE is multiplied by that of IMS. In the future we will focus on improving the sensitivity of the developed technique by employing different online preconcentration techniques preferably implemented directly on the microchip.

Declaration of Competing Interest

There are no conflicts to declare.

Acknowledgements

This work was supported by the Slovak Research and Development Agency (APVV-17-0318 and APVV-0259-12) and the Slovak Grant Agency for Science (VEGA 1/0787/18). This project has received funding from the European Union's Horizon 2020 research and innovation programme (No. 692335). Instrumental support by MaSaTECH (Bratislava, Slovakia) and Merck (Darmstadt, Germany) is also acknowledged. The authors gratefully acknowledge Michal Ďurian for his assistance with preparing 2D plots.

References

[1] Á. Ríos, M. Zougagh, M. Avila, Miniaturization through lab-on-a-chip: utopia or reality for routine laboratories? A review, Anal. Chim. Acta 740 (2012) 1–11.
[2] E.R. Castro, A. Manz, Present state of microchip electrophoresis: state of the art and routine applications, J. Chromatogr. A 1382 (2015) 66–85.
[3] K. Uchiyama, H. Nakajima, T. Hobo, Detection method for microchip separations, Anal. Bioanal. Chem. 379 (2004) 375–382.
[4] M.E. Johnson, J.P. Landers, Fundamentals and practice for ultrasensitive laser-induced fluorescence detection in microanalytical systems, Electrophoresis 25 (2004) 3513–3527.
[5] J.J. Mark, R. Scholz, F.M. Matysik, Electrochemical methods in conjunction with capillary and microchip electrophoresis, J. Chromatogr. A 1267 (2012) 45–64.
[6] M.H. Ghanim, M.Z. Abdullah, Integrating amperometric detection with electrophoresis microchip devices for biochemical assays: recent developments, Talanta 85

(2011) 28–34.
[7] S. Götz, U. Karst, Recent developments in optical detection methods for microchip separations, Anal. Bioanal. Chem. 387 (2007) 183–192.
[8] Y. Liu, X. Huang, J. Ren, Recent advances in chemiluminescence detection coupled with capillary electrophoresis and microchip capillary electrophoresis, Electrophoresis 37 (2016) 2–18.
[9] H. Yang, X.C. Li, F. Yang, J. Feng, M.Y. Lin, Z.G. Chen, Electrochemiluminescence detection system for microchip capillary electrophoresis and its application to pharmaceutical analysis, Microchim. Acta 175 (2011) 193–199.
[10] P.J. Viskari, J.P. Landers, Unconventional detection methods for microfluidic devices, Electrophoresis 27 (2006) 1797–1810.
[11] F. Kitagawa, K. Otsuka, Recent progress in microchip electrophoresis-mass spectrometry, J. Pharm. Biomed. Anal. 55 (2011) 668–678.
[12] H. Borsdorf, T. Mayer, M. Zarejousheghani, G.A. Eiceman, Recent developments in ion mobility spectrometry, Appl. Spectrosc. Rev. 46 (2011) 472–521.
[13] D.P. Guo, Y.H. Wang, T.B. Xu, Y. Zhang, L.F. Li, J.K. Chen, et al., Rapid determination of phenylalanine by micro-chip based field asymmetric waveform ion mobility spectrometry technology, Chinese J. Anal. Chem. 44 (2016) 617–624.
[14] A.A. Shvartsburg, R.D. Smith, Protein analyses using differential ion mobility microchips with mass spectrometry, Anal. Chem. 84 (2012) 7297–7300.
[15] X. Zheng, R. Wojcik, X. Zhang, Y.M. Ibrahim, K.E. Burnum-Johnson, D.J. Orton, et al., Coupling front-end separations, ion mobility spectrometry, and mass spectrometry for enhanced multidimensional biological and environmental analyses, Ann. Rev. Anal. Chem. 10 (2017) 71–92.
[16] G.W. Cook, P.T. LaPuma, G.L. Hook, B.A. Eckenrode, Using gas chromatography with ion mobility spectrometry to resolve explosive compounds in the rresence of interferents, J. Forensic Sci. 55 (2010) 1582–1591.
[17] M. Westhoff, P. Litterst, L. Freitag, W. Urfer, S. Bader, J.I. Baumbach, Ion mobility spectrometry for the detection of volatile organic compounds in exhaled breath of patients with lung cancer: results of a pilot study, Thorax 64 (2009) 744–748.
[18] F. Liang, K. Kerpen, A. Kuklya, U. Telgheder, Fingerprint identification of volatile organic compounds in gasoline contaminated groundwater using gas chromatography differential ion mobility spectrometry, Int. J. Ion Mobil. Spectrom. 15 (2012) 169–177.
[19] V. Ilbeigi, M. Sabo, Y. Valadbeigi, S. Matejcik, M. Tabrizchi, Laser desorption-ion mobility spectrometry as a useful tool for imaging of thin layer chromatography surface, J. Chromatogr. A 1459 (2016) 145–151.
[20] C.B. Shumate, H.H. Hill Jr, Coronaspray nebulization and ionization of liquid samples for ion mobility spectrometry, Anal. Chem. 61 (1989) 601–606.
[21] R.W. Hallen, C.B. Shumate, W.F. Siems, T. Tsuda, H.H. Hill Jr, Preliminary investigation of ion mobility spectrometry after capillary electrophoretic introduction, J. Chromatogr. A 480 (1989) 233–245.
[22] X. Jiang, B. Svensmark, L. Deng, Coupling capillary electrophoresis and ion mobility spectrometry via electrospray interface: a preliminary study, Adv. Mat. Res. 160-162 (2011) 1531–1534.
[23] J. Li, R.W. Purves, J.C. Richards, Coupling capillary electrophoresis and high-field asymmetric waveform ion mobility spectrometry mass spectrometry for the analysis of complex lipopolysaccharides, Anal. Chem. 76 (2004) 4676–4683.
[24] X. Liu, Y.Y. Zhao, K. Chan, S.E. Hrudey, X.F. Li, J. Li, Analysis of nitrosamines by capillary electrospray-high-field asymmetric waveform ion mobility spectrometry-MS with programmed compensation voltage, Electrophoresis 28 (2007) 1327–1334.
[25] H.E. Revercomb, E.A. Mason, Theory of plasma chromatography/gaseous electrophoresis - A review, Anal. Chem. 47 (1975) 970–983.
[26] L. Arce, M. Menéndez, R. Garrido-Delgado, M. Valcárcel, Sample-introduction systems coupled to ion-mobility spectrometry equipment for determining compounds present in gaseous, liquid and solid samples, TrAC, Trends Anal. Chem. 27 (2008) 139–150.
[27] X. Zhong, Z. Zhang, S. Jiang, L. Li, Recent advances in coupling capillary electrophoresis-based separation techniques to ESI and MALDI-MS, Electrophoresis 35 (2014) 1214–1225.
[28] M. Sabo, M. Malásková, O. Harmathová, J. Hradski, M. Masár, B. Radjenovic, et al., Direct liquid sampling for corona discharge ion mobility spectrometry, Anal. Chem. 87 (2015) 7389–7394.
[29] B. Graß, A. Neyer, M. Jöhnck, D. Siepe, F. Eisenbeiß, G. Weber, et al., New PMMA-microchip device for isotachophoresis with integrated conductivity detector, Sens. Actuators B Chem. 72 (2001) 249–258.
[30] D. Kaniansky, M. Masár, M. Danková, R. Bodor, R. Rákocyová, M. Pilná, et al., Column switching in zone electrophoresis on a chip, J. Chromatogr. A 1051 (2004) 33–42.
[31] D. Kaniansky, M. Masár, J. Bielčiková, F. Iványi, F. Eisenbeiss, B. Stanislawski, et al., Capillary electrophoresis separations on a planar chip with the column-coupling configuration of the separation channels, Anal. Chem. 72 (2000) 3596–3604.
[32] G.A. Eiceman, E.G. Nazarov, J.A. Stone, Chemical standards in ion mobility spectrometry, Anal. Chim. Acta 493 (2003) 185–194.
[33] D. Kaniansky, M. Masár, J. Bielčíková, Electroosmotic flow suppressing additives for capillary zone electrophoresis in a hydrodynamically closed separation system, J. Chromatogr. A 792 (1997) 483–494.
[34] D. Kaniansky, M. Masár, R. Bodor, M. Žúborová, M. Ölvecká, M. Jöhnck, et al., Electrophoretic separations on chips with hydrodynamically closed separation systems, Electrophoresis 24 (2003) 2208–2227.
[35] D. Kaniansky, M. Masár, J. Marák, R. Bodor, Capillary electrophoresis of inorganic anions, J. Chromatogr. A 834 (1999) 133–178.
[36] ICH harmonised tripartite guideline, validation of analytical procedures: text and methodology Q2(R1), International Conference on Harmonisation of Technical Requirements for Registration of Pharmaceuticals for Human Use (ICH), (2005), pp. 11–12.
[37] M. Sabo, J. Matúška, S. Matejčík, Specific O_2^- generation in corona discharge for ion mobility spectrometry, Talanta 85 (2011) 400–405.
[38] K.M. Ervin, I. Anusiewicz, P. Skurski, J. Simons, W.C. Lineberger, The only stable state of O_2^- is the X $^2\Pi_g$ ground state and it (still!) has an adiabatic electron detachment energy of 0.45 eV, J. Phys. Chem. A 107 (2003) 8521–8529.
[39] M.D. Wessel, J.M. Sutter, P.C. Jurs, Prediction of reduced ion mobility constants of organic compounds from molecular structure, Anal. Chem. 68 (1996) 4237–4243.
[40] H. Gao, W. Niu, Y. Hong, B. Xu, C. Shen, C. Huang, et al., Negative photoionization chloride ion attachment ion mobility spectrometry for the detection of organic acids, RSC Adv. 4 (2014) 63977–63984.
[41] P. Dwivedi, L.M. Matz, D.A. Atkinson, H.H. Hill Jr, Electrospray ionization-ion mobility spectrometry: a rapid analytical method for aqueous nitrate and nitrite analysis, Analyst 129 (2004) 139–144.

Marián Masár is an associate professor at Department of Analytical Chemistry, Faculty of Natural Sciences, Comenius University in Bratislava, Slovakia. He obtained his Ph.D. degree in analytical chemistry in 2000. He has published over 60 papers, which have more than 1200 citations and his research interests include development of new hyphenated techniques based on capillary and microchip electrophoresis.

Jasna Hradski received her Ph.D. degree in analytical chemistry in 2017. She is an assistant professor at Department of Analytical Chemistry, Faculty of Natural Sciences, Comenius University in Bratislava, Slovakia. Her interest field is focused on microchip electrophoresis combined with various detection techniques.

Michaela Nováková obtained her M.Sc. degree at Department of Analytical Chemistry, Faculty of Natural Sciences, Comenius University in Bratislava, Slovakia in 2017. Her research interest is analysis of complex environmental samples by microchip electrophoresis.

Roman Szucs obtained his Ph.D. degree at Department of Organic Chemistry, University of Ghent, Belgium in 1994. He is now working Department of Analytical Chemistry, Faculty of Natural Sciences, Comenius University in Bratislava, Slovakia as a lecturer. He has published over 60 papers with more than 1500 citations and his current research interests are hyphenated separation techniques and computational methods in analytical chemistry.

Martin Sabo obtained his Ph.D. degree at Department of Experimental Physics, Faculty of Mathematics, Physics and Informatics, Comenius University in Bratislava, Slovakia in 2010. He has published over 30 papers with more than 200 citations and his current interest field is focused on research, development and production of (miniaturized) instrumentation for ion mobility spectrometry and mass spectrometry.

Štefan Matejčík is a professor at Department of Experimental Physics, Faculty of Mathematics, Physics and Informatics, Comenius University in Bratislava, Slovakia. He obtained his Ph.D. degree in 1998 and he has published over 240 papers, which have more than 2500 citations. His current research interests are ion physics and chemistry of plasma, ion mobility spectrometry and mass spectrometry.